Material Damping of Simple Structures in a Simulated Space Environment

Donald L. Edberg*
Stanford University, Stanford, California

The need for accurate, quantitative knowledge of the vibration dissipation of large space structures is explained. The sources of experimental error in vibrational measurements are detailed. A new method for such testing based on the use of a miniature telemetry system is presented, which allows the testing of structures in a simulated space environment consisting of free-fall inside of a vacuum chamber. Theoretical relations are given for the damping ratios of metals and composites. Measured damping ratios for both aluminum and composite beams and plates, and aluminum planar trusses, are presented. Experimental results are used to evaluate the theoretical damping relations.

Nomenclature

b = beam width
C_D = beam drag coefficient
C_V = specific heat per unit mass at constant volume
E = Young's modulus
E_1, E' = storage or elastic modulus of elasticity
E_2, E'' = loss modulus of elasticity
EI = beam bending stiffness
g = structural damping coefficient
h = specimen thickness
I = moment of inertia of section
k = specimen thermal conductivity
ℓ = beam length
M_{tot} = $M_{\text{conc.mass}} + M_{\text{beam}}$
Q = quality factor
T = absolute temperature
V = beam velocity through viscous medium
$V_{(\ )}$ = volume fraction of ( )
α = thermal expansion coefficient
γ = loss angle
δ = logarithmic decrement
ζ = critical damping ratio of oscillation
ζ_v = viscous (atmospheric) damping ratio
η = loss factor
λ = $(\rho\omega^2\ell^4/EI)^{1/4}$
λ_n = root of Eq. (1)
μ = $M_{\text{conc.mass}}/M_{\text{beam}}$
ν = Poisson ratio
ρ = mass density of beam
ρ_{atm} = mass density of atmosphere
σ = damping exponent
τ = relaxation time, Eq. (5)
ψ = specific damping capacity
ω, ω_n = natural frequency
ω_R = $1/\tau$, relaxation frequency
ω_1, ω_2 = half-power bandwidth endpoints

Subscripts

f = composite fiber
m = beam/mass system, Eq. (2)
m = composite matrix, Eqs. (8-16)

Received Feb. 14, 1985; revision submitted May 29, 1985.

*Research Assistant, Department of Aeronautics and Astronautics; currently Member Technical Staff, Applied Technologies Section, Jet Propulsion Laboratory, California Institute of Technology, Pasadena, CA. Member AIAA.

I. Introduction

THE study of various forms of damping has been taking place for nearly as long as vibration itself has been analyzed. Even though the design of current spacecraft has become more routine, the study of damping has taken on increased importance. With the planning of large orbiting platforms and space stations, a thorough knowledge of damping is mandatory. Not only will these structures be larger than any previously orbited, they will be flimsier than ever before. Even with the introduction of active controls, at some frequency the effectiveness of these controls is diminished, and passive damping must be relied upon for vibration dissipation. Indeed, some active control schemes are known to transfer vibrational energy to frequencies above their so-called bandwidth; this phenomenon is known to control engineers as spillover. With all these considerations, it cannot be denied that a quantitative knowledge of passive damping is necessary.

This paper is restricted to the topic of *material* damping. A new and unique method for data acquisition from a freely vibrating structure in free-fall is presented. In addition, remote-controlled equipment has been designed and constructed to manipulate test specimens easily in a vacuum environment. A fairly large representation of materials and geometries has been tested in order to broaden the damping properties and measurements available. A new theory for the prediction of composite damping is introduced.

II. Experimental Damping Measurement

In many vibration tests, there are often questions about the exact boundary conditions that occur. For example, clamped supports may not be truly clamped, as the clamp itself may vibrate. Similarly, a specimen suspended at its nodal points is also open to question, where possible interactions between the axial stress due to hanging and the vibrations may exist, as well as uncertainties in the exact nodal locations. Vibrational measurements employing optical techniques must be used to avoid further interference with the specimen. Other difficulties relating to suspended structures have also been given by Hanks and Pinson.[1]

One has also to consider the effect of atmospheric damping, which has been shown by the author to be as large as or larger than the material damping measured in vacuum in some cases.[2] Its interference may be eliminated by performing the vibration testing in vacuum.

To eliminate the problems of supports and atmosphere leaves free-fall in vacuum as a possible means of vibration testing. Free-fall has been employed previously by experimenters at the MIT Space Systems Laboratory[3-7] in

measurements of aluminum and graphite/epoxy beam damping. All these investigations took place in a vacuum chamber, which had a launcher placed inside. The launcher lofted the specimens into free-fall and, at the same time, excited their vibrations. The vibration levels were measured by a strain gage bonded to the surface of the specimens. The signals from the strain gages were obtained through wires that trailed the specimen during its free-fall period. Later investigations by Sheen and Crawley[6,7] employed a complicated "following mechanism" to keep the length of the trailing wires as small as possible. However, even when the drag caused by the atmosphere was eliminated, there remained a question about the wires. In addition, only one-dimensional structures could be conveniently tested.

This paper presents a new method of vibration testing in free-fall, which eliminates the questions about damping caused by supports, atmosphere, and trailing wires. Instead of attaching wires to relay vibrational signals, our method employs a lightweight, very compact telemetry system, which broadcasts the vibrational data to a ground-based receiver. The effect of the additional mass on the specimens may be easily accounted for in the calculation of damping.[2] The use of the telemetry system allows the testing of any structure geometry, provided it can fit inside the vacuum chamber and can be launched into free-fall. In addition, some unique hardware was developed in order to reset the experiment by remote control without breaking the vacuum.

The data analysis performed in this experiment obtained the damping for all available modes of vibration, unlike the previous experimenters who used a data reduction scheme that filtered out all but the fundamental vibration frequency.[8] Since there is no reason to expect the damping of the higher modes to be any less interesting, we employed a fast Fourier transform method coupled with a "moving block" analysis,[9] which allowed the damping of all modes (within the bandwidth of the method) to be obtained.

As we have said earlier, one of the main purposes of this work was to measure the material damping of various substances by a nonintrusive means. Since we wished to eliminate as many disturbances caused by the measurement instrumentation as possible, telemetry was chosen to relay the vibrational data back for analysis. This choice led to some interesting design problems and some equally unique solutions. Details of these solutions are given in the author's doctoral dissertation.[2]

Another purpose of our research was to measure the material of a number of composites whose damping could be predicted theoretically, in order to try to check their agreement with those theories. Measurements of aluminum and composite plates were also planned to attempt to verify the two-dimensional vibrational theory given by Lee.[10] Finally, to demonstrate the versatility of our method, two multiple-bay planar trusses were tested. The dimensions and properties of the specimens tested are given in Table 1 and Fig. 13.

III. Testing Procedure

The heart of the telemetry method is the telemetry system itself, whose schematic is shown in Fig. 1. The vibrations of the specimen were detected by a strain gage, then amplified by a micropower instrumentation operational amplifier and input to a microminiature FM transmitter. The miniature transmitter was originally designed for implantation into a biological specimen, and had a mass of less than 0.5. Four 20-mAH nickel-cadmium batteries powered the strain gage, amplifier, and transmitter for more than 8 h before recharging the batteries was necessary. All the components were mounted on a custom-design printed circuit board for protection and compactness.

A spring-powered resettable launcher (shown in Fig. 2) was used both to launch the specimen into free-fall and to excite its vibrations. (Both the compression in the springs and the location of the specimen supports could be changed by the experimenter, to enhance certain modes of vibration and prevent the specimen from hitting the ceiling of the vacuum chamber.)

The transmitter signal was then received and amplified, and tape-recorded for subsequent analysis. In order to save time, a radio-controlled forklift (shown in Fig. 3) was used to replace the test specimen back onto the launcher without breaking the vacuum. The launcher's springs were recompressed by remote control. The procedure was repeated until the desired number of tests was completed (normally about 15 per specimen). A diagram of the overall equipment setup is given in Figs. 4a and 4b. The signal generator in Fig. 4a was used to supply an accurate frequency signal because the tape recorder in Fig. 4b was operated at a lower speed due to data reduction system requirements. The vacuum chamber is located in the Thermal Protection Facility at NASA Ames Research Center and was capable of vacuum levels of less than one mm of mercury.

Later, the tape-recorded signal was played back at a lower speed (see Fig. 4b) and digitized by an analog-to-digital converter in the Army Aeromechanics Laboratory at NASA Ames. (Note that the damping ratio of a given signal is un-

Table 1 Specimen dimensions and properties

Sp. No.	Type	Mat'l.	No. ply	2ℓ, mm	w/h, in.	w/h, in.	Mass, g	μ
102	beam	Al	—	784.5	1.867	0.0924	239.6	0.126
103	beam	Al	—	606.0	1.865	0.1222	246.7	0.122
161	plate	Al	—	609.0	16.0	0.090	1569.4	0.019
311	beam	Fg/E	6	637.0	1.728	0.075	98.9	0.305
302	beam	Fg/E	12	633.5	1.939	0.148	215.1	0.140
303	beam	Fg/E	24	630.0	1.942	0.296	426.4	0.071
702	beam	Gr/E	10	636.0	2.007	0.073	93.2	0.324
721	beam	Gr/E	20	634.0	1.729	0.161	163.5	0.185
741	beam	Gr/E	40	632.0	1.230	0.277	217.6	0.139
761	plate	Gr/E	20	609.0	16.0	0.036	715.3	0.042
501	beam	K/E	12	635.0	1.750	0.072	66.7	0.453
521	beam	K/E	24	643.5	1.747	0.148	129.9	0.233
541	beam	K/E	48	636.0	1.257	0.290	199.9	0.151
561	plate	K/E	24	609.0	24.0	0.090	1201.6	0.025
22-bay	truss	Al	—	1378.5	2.61	0.375	418.7	0.072
5-bay	truss	Al	—	1257.3	10.10	0.375	647.9	0.047

NOTE: Al = Aluminum; Gr/E = Graphite/Epoxy; Fg/E = Fiberglass/Epoxy; K/E = Kevlar/Epoxy.

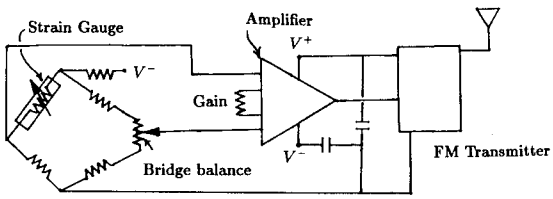

TELEMETRY SCHEMATIC

Fig. 1 Telemetry system schematic.

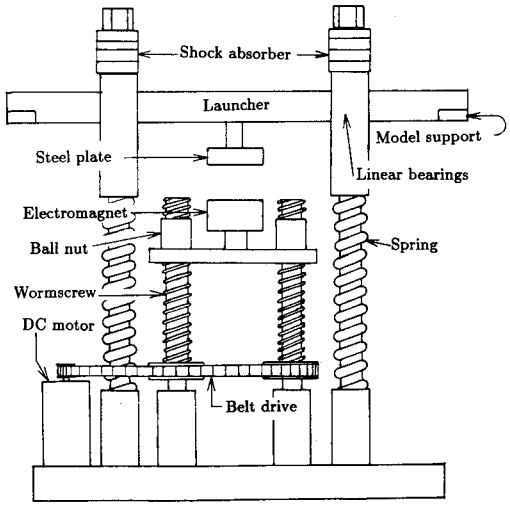

RESETTABLE LAUNCHER

Fig. 2 Specimen launcher.

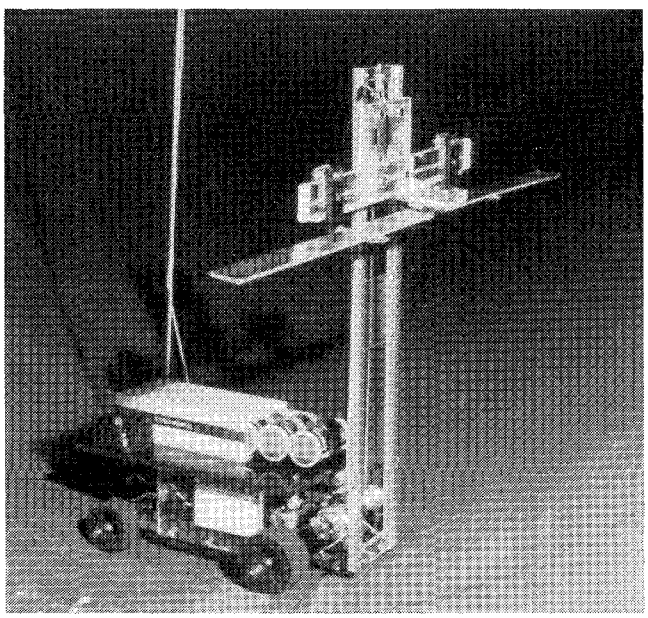

Fig. 3 Radio-controlled forklift.

changed by a reduced playback speed.) It was then input to a computer program called FLT, which used the "moving block" analysis[9] to determine the damping ratio. Any mode appearing on the frequency spectrum of the signal could be analyzed in this manner. A standard error analysis determined that the maximum random error in the damping measurements was about 2.5%. The systematic error in the damping ratios was an estimated 1%.

Considerable effort was put into the design of the mounting for the telemetry system. Since the main form of vibration was expected to be bending vibration of the specimen, the mount had to allow bending without restriction. Other necessary qualities of the mounting system were rigidity, light weight, sturdiness, and ease of positioning or relocating. The telemetry system was placed inside a small plastic case for its own protection and for ease of mounting. After some difficulties with the original mounting system design which may have resulted in damage to the specimen (see Sec. V C), the geometry shown in Fig. 5 was chosen. An aluminum trapezoid was bonded to the plastic case with a screw protruding. The screw was inserted into a small hole drilled through the specimen. Another trapezoid was secured onto the screw with a locknut, which completed the assembly. The telemetry mount allowed bending in one direction and caused no problems in the subsequent testing. The total weight of the telemetry system, case, and mounting hardware was 30 g. The damping ratio is corrected for the additional mass of the telemetry system in Sec. IV B. The mass ratios for the different test specimens are given in Table 1 as the parameter μ.

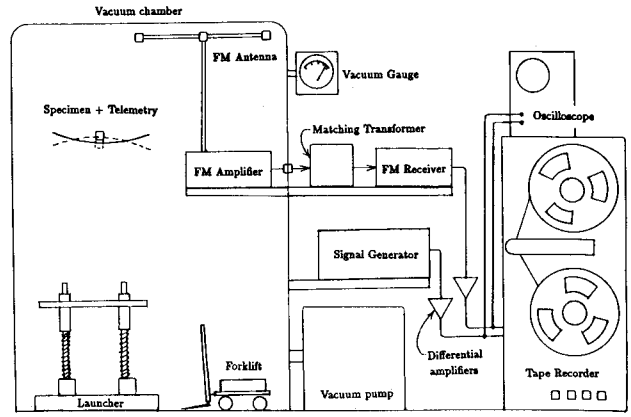

Fig. 4a Data acquisition.

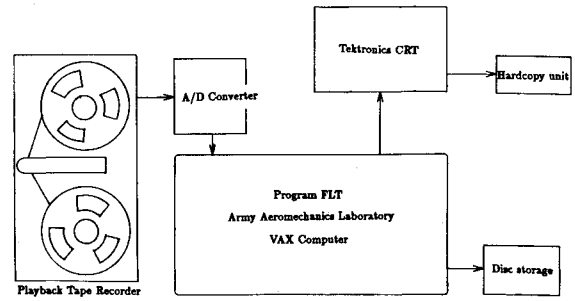

Fig. 4b Data playback and analysis.

IV. Theory

A. Damping Variables

Unfortunately, with the large number of studies of damping, there seem to be nearly as large a number of variables used to describe its values. In order to present a "standard" definition of damping, as well as to be able to compare results easily with recent research from MIT's Space Systems Laboratory,[6,7] we adopt the use of the modal damping ratio ζ as the measure of damping. A comparison of all the different damping variables follows. It is assumed that $\zeta \ll 1$, i.e., small damping.

$$\zeta = \frac{g}{2} = \frac{\eta}{2} = \frac{\delta}{2\pi} = \frac{\tan\gamma}{2} = \frac{\psi}{4\pi} = \frac{-\operatorname{sgn}(\sigma)}{\sqrt{1+(\omega/\sigma)^2}} \cong -\frac{\sigma}{\omega}$$

$$\zeta = \frac{\omega_2 - \omega_1}{2\omega_n} = \frac{1}{2Q} = \frac{E_2}{2E_1} = \frac{E''}{2E'}$$

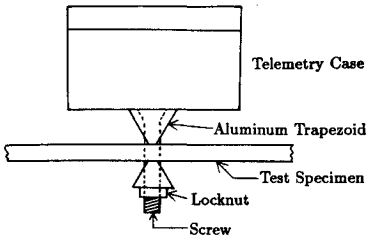

Fig. 5 Telemetry system mount.

B. Effects of Concentrated Mass on Vibrations

The specimen with the telemetry system attached was modeled as a beam with a concentrated mass at its center. It has been shown[2] that the symmetric eigenvalues λ_n of such a system can be determined from calculating the roots of

$$\sin\lambda_n\cosh\lambda_n + \cosh\lambda_n\sinh\lambda_n + \lambda_n\mu(1+\cos\lambda_n\cosh\lambda_n) = 0 \tag{1}$$

where $\mu = M_{\text{conc.mass}}/M_{\text{beam}}$ and $\lambda = (\rho\omega^2\ell^4/EI)^{1/4}$. Here ρ is the mass density of the beam, ω the vibrational frequency, ℓ the length of the beam, and EI the beam bending stiffness. If the damping is assumed to be linear and small, it is possible to show that

$$\zeta = \left(\frac{\lambda_m}{\lambda}\right)^2 \zeta_m \tag{2}$$

In Eq. (2) the subscripted variables refer to the properties of the beam/mass system, while the unsubscripted variables refer to the beam alone. With the eigenvalues shown in Fig. 6, it is possible to convert the damping ratios obtained from the vibrating beam/mass to those of the beam alone.

C. Atmospheric Damping

Included in this paper is a description of the measurement of atmospheric dissipation, or viscous damping. Blevins[11] gives a relation that in this case is modified to read

$$\zeta_v = \frac{1}{2}\left(\frac{\rho_{\text{atm}} b^2}{m_{\text{tot}}/\ell}\right)\left(\frac{V}{\omega b}\right) C_D \tag{3}$$

Here ρ_{atm} is the atmospheric density, b the beam width, V the velocity of the beam through the atmosphere, m_{tot}/ℓ the beam linear density, C_D the beam drag coefficient, and ω the vibrational frequency. According to Eq. (3), the viscous damping ratio is proportional to the atmospheric density and the drag coefficient. For a given beam, we would expect the atmospheric damping to be proportional to the density of the air, which is proportional to the pressure. This conclusion apparently disagrees with the measurements of Vorlicek,[3] who used a free-free aluminum beam in free-fall for similar measurements obtaining a somewhat parabolic curve. We will present our own results for this measurement later.

D. Theoretical Damping of Metals

We will now present theoretical damping models for the materials we tested. Zener[12] proposed that a mechanism causing energy dissipation in metals was heat flow due to strain-induced temperature gradients. His theory produced the following result (for a more rigorous derivation, the reader is referred to the work of Ashley[13]):

$$\zeta = \left(\frac{\alpha^2 ET}{2\rho C_v}\right)\frac{\omega\tau}{1+(\omega\tau)^2} \tag{4}$$

where the relaxation time τ is given by

$$\tau = \frac{\rho C_v h^2}{k\pi^2} \tag{5}$$

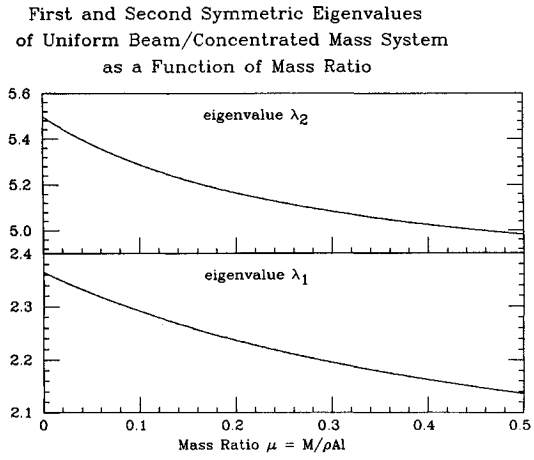

Fig. 6 Eigenvalues of beam/mass system.

Here α is the thermal expansion coefficient, E Young's modulus, T the material absolute temperature, C_v material specific heat per unit mass, h the specimen thickness, and k the thermal conductivity. We will refer to Eq. (4) as the Zener equation. The relaxation frequency is shown to be inversely proportional to the square of the specimen thickness. This fact will be used to correlate tests of different aluminum specimens.

The previous equation gives no reason to believe that a change to two-dimensional geometry will produce different damping. A look at the physical situation, however, suggests that this is not the case. First, the thermal gradients are now two-dimensional rather than one-dimensional. In addition, the effect of Poisson's ratio ν was not considered, and this effect causes a change in dimensions where the thermal gradient due to strain is occurring. Lee[10] has considered the elastothermodynamic analysis of damping in great detail and, after considering the full elastic-thermodynamic coupling for vibrations, he gives the following result for the damping ratio of plates:

$$(\zeta_k)_{\text{plate}} \cong \frac{96}{\pi^4}\left(\frac{1+\nu}{1-\nu}\right)\left(\frac{\alpha^2 ET}{2\rho C_v}\right)\frac{\omega\tau}{1+(\omega\tau)^2} \tag{6}$$

It is useful to note that Lee's analysis yields a result in the form of the Zener equation (4), with a new multiplicative factor. If a plate and a beam are made of the same substance, the maximum damping ratios may be compared as follows:

$$(\zeta)_{\text{max plate}} \cong \left[\frac{1+\nu}{1-\nu}\right](\zeta)_{\text{max beam}} \cong \frac{9}{5}(\zeta)_{\text{max beam}} \tag{7}$$

where we have used $\nu \cong 2/7$ for the Poisson ratio. Lee further notes that the damping of a structure is strongly dependent on the mode shape.

E. Theoretical Damping of Composites

The nature of composite materials makes their analysis follow a different path than the one used for metallic materials. The Zener formula predicts values of the damping ratio that are orders of magnitude smaller than those actually measured, mainly because of differences in thermal conductivity as compared to metals. Thus, we expect that the damping of composites is governed by a different phenomenon.

There are many variables in the fabrication of composites, including fiber orientation, fiber/matrix weight or volume ratio, and fiber type. Each of the many analyses available makes different assumptions as to the mechanics of the damping process. We shall summarize several different

models for the analysis of composite damping. Please note that in all the following derivations, quantities without subscripts are those quantities associated with the *composite*. Quantities related to the fiber or matrix are subscripted f or m, respectively.

The first model introduced is the rule of mixtures.[7] It is assumed that the composite damping ratio is the sum of the products of the volume fractions and damping ratios of the matrix and fiber, that is,

$$\zeta = V_m \zeta_m + V_f \zeta_f \tag{8}$$

A second method is a rule of mixtures weighted by the bending stiffness,[14,15] namely,

$$\zeta = \zeta_f (E_f/E)(I_f/I) + \zeta_m (E_m/E)(I_m/I) \tag{9}$$

In Eq. (9) it is assumed that the composite bending stiffness EI is the sum of the bending stiffnesses of the fiber and matrix, or

$$EI = E_f I_f + E_m I_m \tag{10}$$

and

$$I = I_f + I_m \tag{11}$$

Presumably, one may measure E_m and ζ_m from static and dynamic measurements of a matrix-only specimen.

The third model was proposed by Hashin[16] and is based on a complex modulus concept. The composite was assumed unidirectional; further, it was assumed that the fibers did not contribute to the damping. This results in

$$\zeta = \frac{\zeta_m}{(E_f V_f / E_m V_m) + 1} \tag{12}$$

With this model there seems to be some question about neglecting the fiber's contribution to the damping.

The next method presented here was proposed by Adams and Bacon[17] and includes the effect of shear stress caused by bending. In the model, the total damping ratio is the sum of Eq. (12) and a shear damping ratio. We will not be employing this model for any of our analyses, because results from it are indistinguishable[6] from those obtained from Hashin's model.

Since there is some doubt about neglecting the damping of the fibers, we present another method[2] called full complex stiffness. It is an extension of the Hashin model (12), except that we also include the contribution of the fiber damping. This changes Eq. (12) to

$$\zeta = \frac{\zeta_m + \zeta_f (E_f V_f / E_m V_m)}{1 + (E_f V_f / E_m V_m)} \tag{13}$$

Once the ply damping characteristics are known, either from calculations or experiment, there is still a problem in predicting the damping of a composite whose plies have general orientations. Ni and Adams[18] provide a solution to this problem.

V. Experimental Results

A. Atmospheric Damping

To measure the effects of atmospheric damping, a large number of experimental runs were made at various pressures inside the Heat Transfer vacuum chamber at NASA Ames Research Center's Thermal Protection Facility. The specimen used for this investigation was No. 102 (see Table 1), chosen because of its very prominent first and second modes of vibration.

Figure 7 shows the data obtained, along with the theoretical damping from Eq. (3) added to the average zero-pressure damping and plotted as a continuous line for each of the two modes. As can be easily seen, the data fit the theoretical curves very well. One can see that the data show a linear relationship between damping and atmospheric pressure, as predicted by Eq. (3). It can be observed that the atmospheric damping nearly triples the damping ratio of the first vibrational mode. One can conclude that the atmospheric damping should not be neglected, at least for lightweight specimens.

B. Results for Aluminum Beams

For this series of tests, an additional specimen was fabricated out of a thicker sheet of 2024-T3 aluminum. These experiments were carried out to further validate the test procedure, as there is a large amount of experimental data concerning the material damping of aluminum, which is known to follow the Zener equation (4). Data were obtained at several frequencies, all of which were above the relaxation frequency $\omega_r = 1/\tau$. None were obtained at a frequency lower than ω_r because this required a specimen with such a thin cross section that it could not be launched on the existing launcher without causing very large deflections and resulting high stress levels in the specimen.

Damping ratios were obtained for four different frequencies of vibration, from the first and second modes of each of the two beams. As shown in Fig. 8, all compare very well with the value of ζ predicted by the Zener equation, with the exception of the highest frequency. The reason for the disagreement of the highest frequency measurement is not clear. However, taken as a whole, the data agree well with the theoretical predictions, within experimental error. We thus had confidence that the method could be applied to all the testing we had planned and that the results obtained were equally as good or better than those obtained previously. In addition, the measurements were quite repeatable, as can be seen in the standard deviation bars and the extreme value symbols drawn on Fig. 8.

C. Results for Graphite/Epoxy Beams

For this part of the experiment, three different unidirectional specimens of graphite/epoxy were fabricated with 10, 20, and 40 plies of Fiberite T300 graphite prepreg by the Boeing Aerospace Company. Data were obtained at four different frequencies of vibration. The 10-ply specimen had two significant modes, but the data analysis for the low-frequency mode was abnormally poor and was thus discarded, leaving usable measurements of damping at three frequencies for the three specimens.

The data show remarkable consistency, all having a coefficient of variation of less than ± 0.07 (the coefficient of variation is defined as the ratio of the standard deviation to

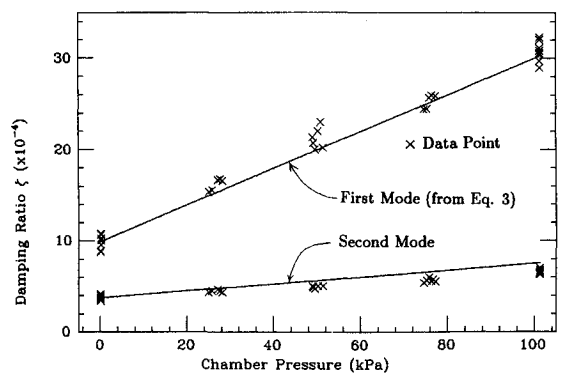

Fig. 7 Damping ratio vs pressure.

the mean). The extreme values measured were all within ±12.5% of the mean, a narrow envelope. These results are plotted in Fig. 9. They compare well with the damping ratios presented by Sheen and Crawley,[6,7] with the exception of the present data, which have smaller scatter. There seems to be no damping dependence on the number of plies of the graphite fibers because the measured values for 10, 20, and 40 plies are all close to each other and close to those values measured by Sheen and Crawley[6,7] for different 8-ply specimens.

One other aspect of the testing of the graphite specimens is worth mentioning. During the initial testing of the thinnest specimen, the measured damping doubled over two successive launches. Close examination of the specimen after the testing indicated that two lengthwise cracks had developed near the center of the specimen, probably from successive impacts onto the vacuum chamber floor. A plot of the damping ratio vs the launch number is shown in Fig. 10. One can speculate that the damage to the specimen occurred after the tenth launch, because the damping suddenly rises between the tenth and eleventh launch. What this apparently means is that the occurrence of this sort of damage may possibly be ascertained solely by inspection of the damping ratio time history. This fact might be very useful to on-orbit evaluation of the condition of large space structures. (The initial damping level in Fig. 10 is higher than that in Fig. 9 because the telemetry mount was redesigned after the damage occurred. The design used for all the subsequent testing is shown in Fig. 5.)

Ni and Adams[18] also tested several graphite specimens, including a unidirectional graphite beam, for which they found a damping ratio of approximately 2.7×10^{-4}. There was no frequency given for the test. In addition, this value is significantly less than the damping ratio given for the fibers alone (3.6×10^{-4}), so it is possible that some sort of plotting error may have occurred therein.

D. Results for Fiberglass/Epoxy Beams

Since there is a need for knowledge of the dynamic characteristics of some less expensive composite materials, we examined the damping of fiberglass/epoxy unidirectional composites. Three beams were fabricated by the Boeing Aerospace Company with 6, 12, and 24 plies from Ferro S-2/CE321R prepreg. Data were obtained at five different frequencies: the 6- and 12-ply specimens had two prominent modes each, while the 24-ply specimen had only one measurable mode of vibration. These data also showed very good consistency, with the maximum coefficient of variation being 10.36% (all of the others were less than 6.4%). All the extreme measurements were within two standard deviations of the mean values. The mean values, standard deviations, and extreme values are all plotted vs frequency of vibration in Fig. 11. It is apparent that there is again little or no dependence of the damping ratio on the number of plies of the specimen. In this case, however, there does seem to be slight dependence on the frequency of oscillation.

E. Results for Kevlar/Epoxy Beams

The motivation for the testing of Kevlar† was provided by an advertisement in *Astronautics and Aeronautics* claiming

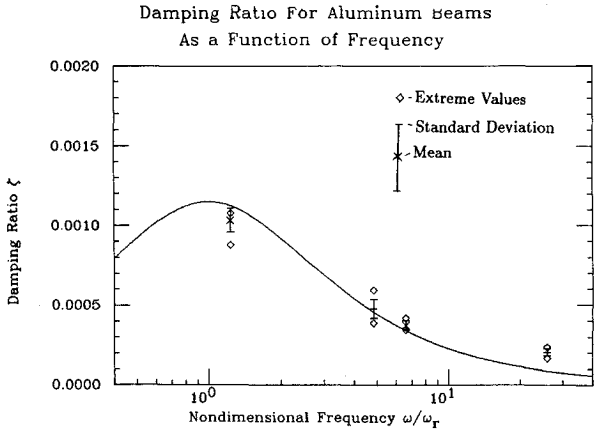

Fig. 8 Damping vs frequency for aluminum beams.

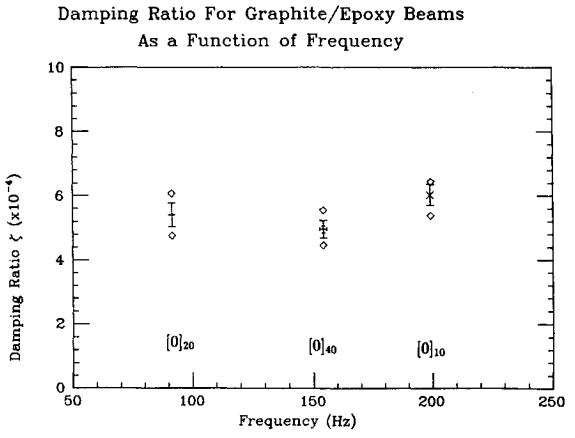

Fig. 9 Damping vs frequency for graphite beams.

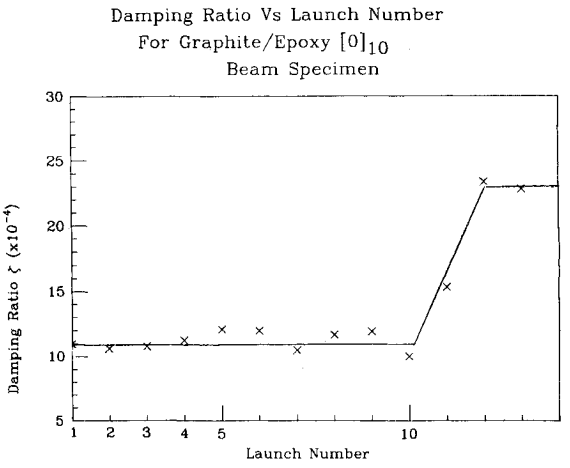

Fig. 10 Damping vs launch number.

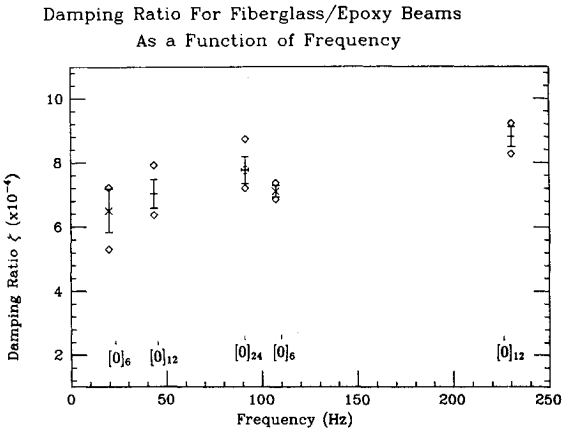

Fig. 11 Damping vs frequency for fiberglass beams.

†Kevlar is a registered trademark of the DuPont Company.

that Kevlar composites had been measured to give several times the damping of other composites.[19] Since we expect that designers will have to use as much passive damping as they can in the design of large space structures, we included Kevlar in our experiments. Three beams were laminated by the Boeing Aerospace Company from 12, 24, and 48 plies of unidirectional preimpregnated fibers obtained from the U.S. Polymeric Corporation. Damping data were obtained at four different frequencies—two for the thinnest specimen, and one each for the other two specimens. These covered a fairly broad frequency range, from 25 Hz up to 160 Hz. The data had a very small scatter; the worst coefficient of variation was less than 0.07. As before, all the mean values, standard deviations, and extreme values are plotted in Fig. 12.

Examination of Fig. 12 reveals that the damping ratio has essentially no dependence on the number of plies in the specimen, or on the vibrational frequency. What is most interesting is that the vertical scale of Fig. 12 has been multiplied by a factor of *ten* as compared to the other composite figures. What this means is that *the damping ratio of unidirectional Kevlar composites is an order of magnitude higher than all the other unidirectional composites tested here.* The large space structure designer should take notice of this interesting fact.

In a literature search, only two references were found, both describing the same experimental measurement of Kevlar damping. Pulgrano and Miner[14] and the DuPont Company[15] used the free vibration technique for their measurements, which tested the Kevlar beams in their cantilever modes in air. Average damping ratios obtained were 0.009, about 80% higher than the values that we obtained. This discrepancy is probably due to a combination of atmospheric dissipation and losses at the cantilever support.

The damping data for all the above composites are summarized in Table 2.

F. Evaluation of the Composite Damping Models

Several theories have been presented for the prediction of composite damping. After rejecting those models that neglect composite fiber damping, three models remain: rule of mixtures, Eq. (8); stiffness rule of mixtures, Eq. (9); and full complex modulus, Eq. (13). Measured damping data were used to compare the predictions of the three models in order to attempt to determine which of these models gave the most realistic damping values. Unfortunately, even with all the component moduli and volume fractions known, there remained *two* unknowns, ζ_m and ζ_f. One further relation was needed to compare the models. In this experiment, it was known that several different composite specimens were fabricated from the same epoxy resin.[20] In this case, it was possible to equate the damping of the resins of the different composites to see which models (if any) led to a contradiction. This operation yielded a relation for the remaining unknowns ζ_f for the two composites.

Equation (8) was solved for ζ_m, and the expression for the two materials were equated, yielding the relation

$$(\zeta_f)_{\text{Kevlar/epoxy}} = 1.14(\zeta_f)_{\text{graphite/epoxy}} + 64.3\times 10^{-4} \quad (14)$$

The manufacturer-supplied properties given in Table 3 were used in this relation, which seems to indicate that the damping ratio of the Kevlar fibers is more than the Kevlar composite damping ratio (average value of 55×10^{-4}), implying a *negative* damping ratio for graphite fibers. Since this is not a possible situation, Eq. (8) is not considered further. Similar operations on Eqs. (9) and (13) yielded

$$(\zeta_f)_{\text{Kevlar/epoxy}} = 1.71\ (\zeta_f)_{\text{graphite/epoxy}} + 35.8\times 10^{-4} \quad (15)$$

and

$$(\zeta_f)_{\text{Kevlar/epoxy}} = 2.11\ (\zeta_f)_{\text{graphite/epoxy}} + 33.6\times 10^{-4} \quad (16)$$

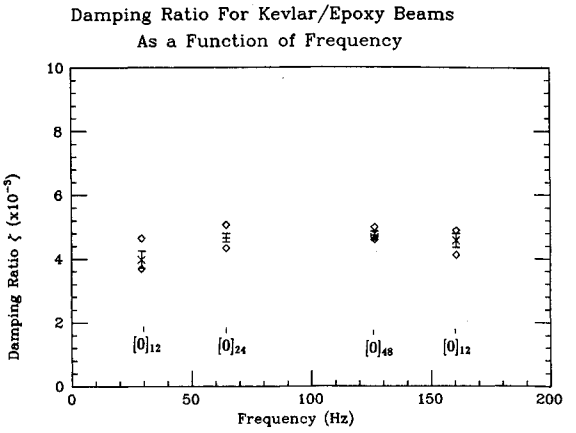

Fig. 12 Damping vs frequency for Kevlar beams.

Table 2 Experimental results—beams

Material	Mean ζ ($\times 10^{-4}$)	ζ Dependence
Aluminum	2.8 to 9.9	Very frequency dep.
Graphite/epoxy	5.4	—
Fiberglass/epoxy	7.7	Slight frequency dep.
Kevlar/epoxy	55.0	—

Table 3 Composite properties (from manufacturers)

Composite	V_f	V_m	E(GPa)	E_f(GPa)	E_m(GPa)
Graphite/epoxy	.63	.37	138	231	3.4
Kevlar/epoxy	.60	.40	77.2	124	3.4

respectively. One can see that both Eqs. (15) and (16) are approximately the same, even though they are based on the use of different material properties. This provides reason to believe that they may provide meaningful results.

As a means of further evaluating Eqs. (9) and (13), we need to input an approximate value for ζ_m. A possibly "good" value for our use is found in Ni and Adams.[18] Although the epoxy resin they experimented with is different from ours, it seems reasonable to believe that its properties will be nearly the same as our resin. In their work, a value of $\psi = 6.54\%$ was given, corresponding to $\zeta_m = 5.2\times 10^{-3}$. Using this value in Eqs. (9) and (13) gave identical values for Kevlar fiber damping ratio of 4.4×10^{-3} and nearly identical values for the graphite fibers of 5.02 and 5.07×10^{-4}. We repeat, however, that these calculations were based on the matrix properties of a different epoxy resin from the one we used. We believe that those properties are nearly the same as the ones describing our own resin. Based on those assumptions, we feel that Eqs. (9) and (13) give the best estimate of the damping ratio of unidirectional composites at this time. In practice, we feel that the method given by Ni and Adams[18] is likely to be the most useful because it may be used for any ply orientations.

G. Plates—Experimental Results

In order to attempt to verify Lee's theory[10] of plates by experiment and to show the versatility of the telemetry method for the experimental measurement of vibration, several plates of uniform thickness were made from aluminum, graphite/epoxy, and Kevlar/epoxy. Details of the plate testing are given in the author's Ph.D. dissertation,[2] and results are presented in Table 4. For aluminum, the expected value given for ζ was calculated from Eq. (6) using the appropriate material constants and frequency. Subsequent analysis has indicated that the aluminum plate was

vibrating below its relaxation frequency ($\omega/\omega_R \approx 0.3$). Sheen and Crawley[7] have shown that the damping ratio of aluminum is not independent of stress level at such frequencies. Since the stress level was not regulated in the current work, this phenomenon may have contributed to the disagreement in the first line of Table 4. "Oilcanning" is also believed to have affected the results for aluminum. The composite plate damping ratios are believed to be higher than the unidirectional values given earlier simply because the composite plates were laminated from alternating 0 and 90° plies. This construction is known to have higher damping than unidirectional layups.

H. Planar Lattices—Experimental Results

As a final use of the telemetry method to determine experimentally the damping of simple structures, two multibay planar trusses were borrowed from MIT and tested. Each was machined from a single piece of aluminum; one had 5 repeating substructures (bays), while the other had 22 bays. These planar trusses are shown in Fig. 13. As might be expected, with structures of this complexity, the frequency spectrum was "mode-rich." Within the bandwidth of the analysis program, there were at least five or six recognizable modes. The damping of the modes of the 22-bay truss may be seen in Fig. 14. The solid line is the Zener damping [Eq. (4)] based on the thickness of the longer members. It is clear that this simple law does not properly describe the energy dissipation for any of the modes we measured. Clearly, a complicated system like the truss must be analyzed by a more realistic model. We know of no such model, finite element or otherwise, which permits the damping to be calculated *from* the motion of the structure.

Table 4 Experimental results—plates

Material	Measured ζ ($\times 10^{-4}$)	Expected ζ ($\times 10^{-4}$)
Aluminum	36.1	18.3
Graphite/epoxy	51.8	—
Kevlar/epoxy	75.5	—

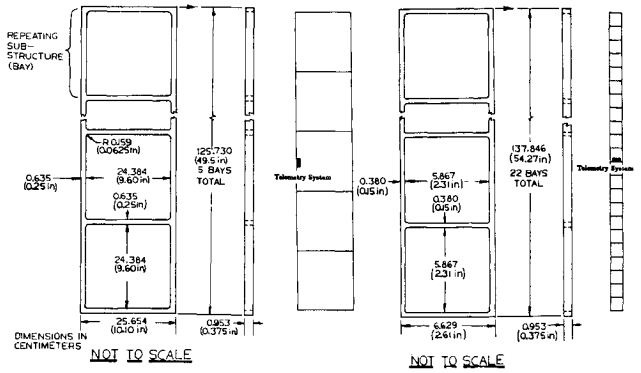

Fig. 13 5- and 22-bay planar trusses.

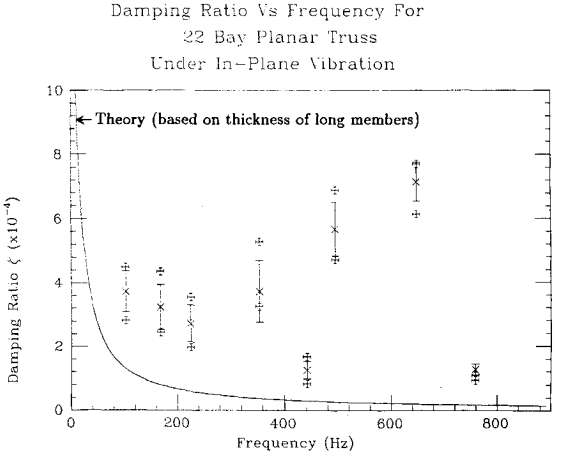

Fig. 14 Damping vs frequency for 22-bay planar truss.

VI. Conclusions

Several new ideas have been introduced in this paper. From the data collected, the following conclusions are made:

1) The telemetry method has been shown to be useful and practical for the free-fall testing of arbitrary structures, including beams, plates, and trusses.

2) More work is needed to accurately determine the effect of Poisson's ratio on the thermoelastic damping of materials. It may be that this effect is overshadowed by more dominant effects.

3) The rule of mixtures based on volume fractions theory for composite damping leads to impossible results. The other two theories seem to be much better, as they yield comparable results even though they are based on the use of different material properties.

4) The damping caused by the atmosphere may not be negligible and should be accounted for in the measurement of damping.

5) The damping values of aluminum may be used as a means of determining the accuracy of damping measurements, as they have repeatedly been shown to follow the Zener relation.

Acknowledgments

This work was performed while the author was a research assistant for the Department of Aeronautics and Astronautics at Stanford University, Stanford, CA. The research was supported by the Air Force Office of Scientific Research under Contract AFOSR 82-0062. The author is grateful for advice and discussions with Professor Holt Ashley, his dissertation advisor. In addition, the author wishes to thank Mr. Bill Walker of the Boeing Aerospace Company, who provided all the composite specimens that were tested; Professor James Williams Jr. at MIT for lending the planar trusses for testing; Messrs. Seth Dawson and Bob George of the Army Aeromechanics Laboratory, who provided the data reduction software and hardware; and Messrs. Roy Wakefield and Fred Bear of the Thermal Protection Facility at NASA Ames Research Center, who provided the use of the vacuum chamber. In addition, the author wishes to thank his good friends Ofer Bruhis and Brian Chan for their assistance in the fabrication of some of the experimental hardware.

References

[1]Hanks, B. R. and Pinson, L. D., "Large Space Structures Raise Testing Challenges," *Astronautics and Aeronautics*, Vol. 21, Oct. 1983, pp. 34-40.

[2]Edberg, D., "Measurement of Material Damping in a Simulated Space Environment," Ph.D. Dissertation, Dept. of Aeronautics and Astronautics, Stanford University, Stanford, CA, Dec. 1984.

[3]Vorlicek, P. L., "Material Damping of Aluminum and Graphite/Epoxy in a Simulated Zero-Gravity Environment," MIT Space Systems Laboratory, Cambridge, MA, Rept. 13-81, Jan. 1981.

[4]Crawley, E. F. and Mohr, D. G., "Experimental Measurements of Material Damping in Free-Fall with Tuneable Excitation," AIAA Paper 83-0858 NV, May 1983.

[5]Mohr, D. G. and Crawley, E. F., "Experimental Measurements of Material Damping of Aluminum and Graphite/Epoxy in Free-Fall with Tuneable Excitation," MIT Space Systems Laboratory, Cambridge, MA, Rept. 11-82, June 1982.

[6]Sheen, R. F. and Crawley, E. F., "Experimental Measurement of Material Damping for Space Structures," presented at the Vibration Damping Workshop, Long Beach, CA, Feb. 1984.

[7]Sheen, R. F. and Crawley, E. F., "Experimental Measurement of Material Damping for Space Structures in Simulated Zero-G," MIT Space Systems Laboratory, Cambridge, MA, Rept. 1-84, Dec. 1983.
[8]Marquardt, D. W., "An Algorithm for Least-Squares Estimation of Nonlinear Parameters," *Journal of the Society for Industrial and Applied Mathematics,* Vol. II, June 1963, pp. 431-441.
[9]Bousman, W. G. and Winkler, D. J., "Application of the Moving Block Analysis," *Proceedings of the AIAA/ASME/ASCE/AHS 22nd Structures, Structural Dynamics, and Materials Conference, Atlanta, GA,* April 1981, pp. 755-763.
[10]Lee, U., "Thermal and Electromagnetic Damping Analysis and Its Application," Ph.D. Thesis, Dept. of Mechanical Engineering, Stanford University, Stanford, CA, Aug. 1984.
[11]Blevins, R. D., *Flow-Induced Vibration,* Van Nostrand Co., New York, 1977, pp. 218-220.
[12]Zener, C. M., *Elasticity and Anelasticity of Metals,* University of Chicago Press, Chicago, IL, 1948.
[13]Ashley, H., "On Passive Damping Mechanisms in Large Space Structures," *Journal of Spacecraft and Rockets,* Vol. 21, Sept-Oct. 1984, pp. 448-455.
[14]Pulgrano, L. J. and Miner, L. H., "Effects of Fiber and Resin on the Vibration Damping of Composites Reinforced With Fiberglass, Graphite, and Aramid," *Proceedings of the 28th SAMPE Meeting,* Anaheim, CA, April 1983.
[15]"Vibration Damping of Kevlar 49 Aramid, Graphite, and Fiberglass Fibers and of Composites Reinforced With These Fibers," DuPont Co., Wilmington, DE, PIM 428, Nov. 1981.
[16]Hashin, Z., "Complex Moduli of Viscoelastic Composites-II. Fiber Reinforced Materials," *International Journal of Solids and Structures,* Vol. 6, 1970, pp. 797-807.
[17]Adams, R. D. and Bacon, D. G. C., "Measurement of the Flexural Damping Capacity and Dynamic Young's Modulus of Metals and Reinforced Plastics," *Journal of Physics D: Applied Physics,* Vol. 6, Jan. 1973, p. 27.
[18]Ni, R. G. and Adams, R. D., "The Damping and Dynamic Moduli of Symmetric Laminated Composite Beams—Theoretical and Experimental Results," *Journal of Composite Materials,* Vol. 18, Mar. 1984, pp. 104-121.
[19]Langston, P. R., "Designing with Advanced Composites," Advertisement, *Astronautics and Aeronautics,* Vol. 21, Oct. 1983, p. 15.
[20]Reilly, D., private communication from the Boeing Aerospace Co., Seattle, WA, May 1984.